Specific Cleavage of a DNA Triple Helix by Fe^{II}·Bleomycin†

Stefanie A. Kane,‡ Sidney M. Hecht,*,‡ Jian-Sheng Sun,§ Thérèse Garestier,§ and Claude Hélène§

Departments of Chemistry and Biology, University of Virginia, Charlottesville, Virginia 22901, and Laboratoire de Biophysique, Muséum National d'Histoire Naturelle, INSERM U201, CNRS URA 481, 43 rue Cuvier, 75231 Paris Cedex 05, France

Received August 17, 1995; Revised Manuscript Received October 25, 1995⊗

ABSTRACT: The specific cleavage of a DNA triple helix by Fe^{II}·bleomycin (BLM) is demonstrated. Triplex-specific cleavage was observed on both strands of the 32-base pair (bp) duplex at the duplex−triplex junctions. Strand scission products and alkali labile lesions were both formed. The strongest BLM cleavage site was located at the 5′-duplex−triplex junction, which is also the preferred triplex binding site of intercalating agents [Collier, D. A., Mergny, J.-L., Thuong, N. T., & Hélène, C. (1991) *Nucleic Acids Res. 19,* 4219−4224]. The preference of BLM for the 5′-junction does not appear to derive from selective intercalative binding at this site. This is supported by the observation that phleomycin, which contains a thiazolinylthiazole moiety rather than a planar bithiazole ring system, exhibited the same selectivity of triplex cleavage as BLM. Cleavage of the triple helix by Fe^{II}·BLM was unaffected by concentrations of Mg^{2+} up to 5 mM, suggesting possible therapeutic applications of this novel DNA target. Molecular-modeling calculations of the triplex region suggested that dramatic variations in minor groove width and depth occur at the duplex−triplex junctions, particularly at the 5′-junction. Moreover, the minor groove at these sites was calculated to be somewhat shallower and wider than the minor groove of B-DNA. These results suggest that the preference of BLM for the duplex−triplex junctions derives from selective recognition of minor groove shape at these sites and thus reflects conformation-selective, rather than sequence-selective, DNA recognition by Fe^{II}·BLM.

The bleomycins (Figure 1) are a family of antitumor antibiotics used clinically for the treatment of several neoplastic diseases (Sikic et al., 1985). BLM[1] oxidatively degrades both DNA (Hecht, 1986, 1995; Stubbe & Kozarich, 1987; Natrajan & Hecht, 1993; Kane & Hecht, 1994) and RNA (Carter et al., 1990; Holmes et al., 1993; Hecht, 1994) in the presence of redox active metals, such as Fe (Sausville et al., 1978) or Cu (Ehrenfeld et al., 1987), and molecular oxygen. Fe^{II}·BLM reductively activates oxygen to form the ternary complex called activated BLM (Burger et al., 1981; Hecht, 1986; Stubbe & Kozarich, 1987). Two sets of DNA degradation products have been identified, both of which are believed to derive from a common reactive DNA intermediate (Wu et al., 1985; Kozarich et al., 1989). One intriguing aspect of the action of BLM is its selective recognition of $^{5'}GC^{3'}$ and $^{5'}GT^{3'}$ sequences within B-form DNA (D'Andrea & Haseltine, 1978; Takeshita et al., 1978). Substantial research efforts have been focused on systematic structural variation of the BLM molecule in an attempt to define the structural requirements for BLM activation and DNA recognition by BLM [reviewed in Natrajan and Hecht (1993)].

In addition to BLM structure, the structure of the nucleic acid target has been shown to influence the sites recognized by BLM. Alteration of DNA structure by platination (Mascharak et al., 1983; Gold et al., 1988), by methylation (Hertzberg et al., 1985; Long et al., 1990), or by the introduction of bulges (Williams & Goldberg, 1988) resulted in novel BLM-induced cleavage patterns. An early finding that demonstrated the recognition of DNA conformation by BLM was the observation that treatment of plasmid DNAs with limited amounts of BLM led to the production of small numbers of unique cleavage sites localized within a discrete region of the DNA molecule (Haidle et al., 1979). In a related study, the effects of the topological state of plasmid DNA molecules on the selectivity of strand scission were investigated (Mirabelli et al., 1983). A number of cleavage sites induced in a supercoiled DNA were not observed in the corresponding linearized DNA substrate, suggesting that the selectivity of BLM-mediated DNA degradation was

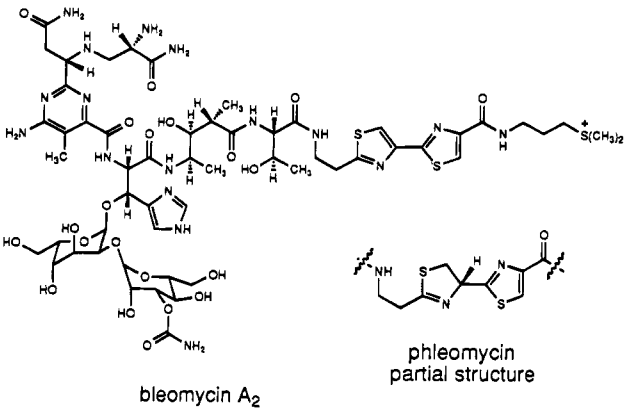

FIGURE 1: Structure of bleomycin A_2 and a partial structure showing the structural difference between bleomycin and phleomycin.

† This work was supported at the University of Virginia by National Institutes of Health Research Grant CA53913, awarded by the National Cancer Institute, and at the Muséum National d'Histoire Naturelle by a visiting professorship to S.M.H.

* Author to whom correspondence should be addressed.

‡ University of Virginia.

§ Muséum National d'Histoire Naturelle.

⊗ Abstract published in *Advance ACS Abstracts,* December 1, 1995.

[1] Abbreviations: BLM, bleomycin; Tris, tris(hydroxymethyl)aminomethane; EDTA, ethylenediaminetetraacetic acid; SDS, sodium dodecyl sulfate; bp, base pair; nt, nucleotide; MPE, methidium propyl−EDTA; DTT, dithiothreitol; Phen, phenanthroline.

0006-2960/95/0434-16715$09.00/0

```
3' - AGGACTATTTCCTCCTCTACTTCTTTTTTACT - 5'
5' - TCCTGATAAAGGAGGAGATGAAGAAAAAATGA - 3'
        5' - TTTCCTCCTCT - 3'
```

FIGURE 2: Sequence of the DNA triple helix employed as a substrate for Fe^{II}·BLM. The numbering of the triple helix sequence proceeds from left to right.

influenced by the conformation of the DNA substrate. Recognition of nucleic acid conformation by BLM has also been documented for BLM-mediated degradation of RNA (Carter et al., 1990; Holmes et al., 1993; Hecht, 1994). Although RNA cleavage predominated at $^{5'}$G-Pyr$^{3'}$ sequences, as was also observed for DNA cleavage, cleavage of RNA was much more selective than that of DNA. Interestingly, a substantial number of cleavage sites were located at the putative junctions between single- and double-stranded regions of the RNA molecule, suggesting selective recognition of nucleic acid structure by Fe^{II}·BLM, rather than sequence. Further evidence supporting this idea was the observation that NaCl, $MgCl_2$, and spermidine, reagents known to alter RNA conformation, affected the efficiency of RNA cleavage by Fe^{II}·BLM (Holmes et al., 1993). It has also been shown that a tRNA precursor transcript and its corresponding tDNA underwent Fe^{II}·BLM cleavage with the greatest efficiency at the same site, consistent with recognition of nucleic acid conformation (Holmes & Hecht, 1993).

In an effort to further define the source(s) of nucleic acid recognition by Fe^{II}·BLM and to identify unique polynucleotide structures that can serve as potential therapeutic targets, the ability of a DNA triple helix to serve as a substrate for Fe^{II}·BLM was investigated. The ability of Fe^{II}·BLM to cleave such structures, particularly at the 5′-junction, seemed interesting because the 5′-junction has been determined to be the preferred triple helix binding site of intercalating agents. For example, the binding of ellipticine to a triple helix was investigated by the use of a photoinactivatable ellipticine derivative (Perrouault et al., 1990). Photoinduced cleavage of the triplex by this ellipticine analogue was observed on both strands at the 5′-junction. Similarly, diethyl pyrocarbonate (DEPC) footprinting has been used to study the binding of intercalators to a DNA triple helix (Collier et al., 1991a); the intercalators acridine, ellipticine, and propidium iodide all induced DEPC hypersensitivity at the 5′-junction. DEPC alkylates the N-7 position of adenosines; the binding of an oligonucleotide to the major groove of duplex DNA was shown to protect the adenosines within the triple helical region from modification by DEPC. However, intercalation at the junction resulted in a conformational change which exposed the N-7 of the first adenosine at the junction, making it highly susceptible to attack by the alkylating agent. In contrast, echinomycin, actinomycin D, and the minor groove binders DAPI and Hoescht 33342 did not induce DEPC hypersensitivity at the duplex−triplex junction.

The sequence of the triplex employed for this investigation is illustrated in Figure 2. This sequence was chosen because it is known to form a (stable) triplex and because a significant amount of data regarding the structure of this molecule is available (François et al., 1988, 1989a; Sun et al., 1989, 1991). Importantly, the entire sequence is devoid of $^{5'}$G-Pyr$^{3'}$ sequences, those normally recognized in B-DNA by Fe^{II}·BLM. Presently, we demonstrate specific cleavage of the DNA triple helix by Fe^{II}·BLM at sites that reflect recognition of DNA conformation rather than sequence. We also demonstrate that the chemistry of triplex degradation is analogous to that involved in the cleavage of duplex DNA.

EXPERIMENTAL PROCEDURES

Materials. Blenoxane, obtained as a gift from Bristol Laboratories, was fractionated as described (Chien et al., 1977) to yield BLM A_2. Phleomycin (copper-free) was obtained from the Institute of Microbial Chemistry, Tokyo. Methidium propyl−EDTA was kindly provided by Dr. Robert Hertzberg, SmithKline Beecham Pharmaceuticals. T4 polynucleotide kinase was purchased from United States Biochemical. [γ-^{32}P]ATP (7000 Ci/mmol) was obtained from ICN Biomedicals. β-Cyanoethyl phosphoramidites, β-cyanoethyl phosphoramidite activator solution, and CPG 500 Å solid supports were obtained from Milligen/Biosearch. Nensorb columns were purchased from DuPont-New England Nuclear. C_{18} Sep-Pak cartridges were purchased from Waters. Distilled, deionized water from a Milli-Q system was used for all aqueous solutions and manipulations.

Methods. Polyacrylamide gel loading solution consisted of 10 M urea, 1.5 mM EDTA, 0.05% (w/v) xylene cyanol, and 0.05% (w/v) bromphenol blue. Polyacrylamide gel electrophoresis was carried out in 90 mM Tris-borate buffer (pH 8.3) containing 5 mM EDTA. Autoradiography was carried out with Kodak X-Omat film at −80 °C. Storage phosphor autoradiography was carried out at room temperature with Kodak Storage phosphor screens obtained from Molecular Dynamics. A Molecular Dynamics 400S Phosphorimager was used to obtain all information from the storage screens. The data were analyzed by performing volume integrations of the target site and total DNA in a given lane using the ImageQuant version 3.2 software. The oligodeoxynucleotide concentrations in all experiments refer to strand concentration, unless otherwise indicated. Chemical sequencing of the 5′-^{32}P end-labeled oligodeoxynucleotides was carried out using a modification of the Maxam−Gilbert procedure (Jay et al., 1982).

Synthesis and Purification of Oligodeoxynucleotides. Oligodeoxynucleotides were synthesized on a Biosearch model 8600 DNA synthesizer using β-cyanoethyl phosphoramidites (Caruthers, 1985). After cleavage of the synthesized oligonucleotides from the solid support with NH_4OH, each oligomer was detritylated and purified by Nensorb chromatography according to the manufacturer's protocol. Oligodeoxynucleotides were purified further on preparative 20% denaturing polyacrylamide gels. The DNA bands were visualized by UV shadowing and excised from the gel, and the DNA was recovered by electroelution. The DNA solutions were desalted by reversed phase chromatography on C18 Sep-Pak cartridges.

5′-^{32}P End Labeling of 32-mer Oligonucleotides. The oligodeoxynucleotide (1 μg) was 5′-^{32}P end-labeled in a reaction mixture (20 μL total volume) containing 50 mM Tris-HCl (pH 7.6), 1 mM $MgCl_2$, 10 mM β-mercaptoethanol, 0.15 mCi (1 μM) of [γ-^{32}P]ATP, and 6 units of T4 polynucleotide kinase (one unit is the amount of enzyme required to incorporate 1 nmol of phosphate from [γ-^{32}P]-ATP into acid-precipitable material in 30 min at 37 °C). The reaction mixture was incubated for 10 min at 37 °C, and then unlabeled ATP (in reaction buffer) was added to a final

concentration of 2.5 μM and the incubation continued for 30 min. The radiolabeled DNA was purified on a 20% denaturing polyacrylamide gel. The gel was run at 13−15 W for 3 h and then visualized by autoradiography. The bands of interest were excised from the gel, and the DNA was eluted into 0.6 M ammonium acetate containing 0.1 mM EDTA and 0.1% (w/v) SDS and recovered by ethanol precipitation.

Hybridization of Oligonucleotides and Triplex Formation. The complementary 32-mer oligodeoxynucleotides were hybridized in 10 μL (total volume) of 10 mM sodium cacodylate (pH 6.0) containing 100 mM NaCl, 0.5 μM unlabeled strand, and 0.4 μM ^{32}P-labeled strand (2.5×10^6 cpm). The solution was heated at 90 °C for 2 min and then allowed to cool to room temperature over a period of 1 h. Hybridization of the two strands was verified by 20% native polyacrylamide gel electrophoresis.

Triplex formation was accomplished by incubation of the 32 bp DNA duplex (20 nM, 1×10^5 cpm) with the 11-mer oligodeoxynucleotide (20 μM) in a reaction mixture (10 μL total volume) containing 10 mM sodium cacodylate (pH 6.0), 100 mM NaCl, and 0, 0.5, 1, 2, or 5 mM $MgCl_2$, where indicated, at room temperature for 2 h.

Cu^{II}·Phenanthroline Footprinting of the DNA Triple Helix. Reaction mixtures (20 μL total volume) contained 10 nM duplex (1×10^5 cpm) and 10 μM 11-mer in 10 mM sodium cacodylate (pH 6.0) containing 100 mM NaCl, 30 μM 1,10-phenanthroline, 15 μM $CuSO_4$, and 2 mM 3-mercaptopropionic acid. Reaction mixtures were incubated for 30 min at 0 °C, and then the reactions were quenched by the addition of neocuproine (to a final concentration of 1 mM) and 10 μL of gel loading solution. Samples were heated at 90 °C for 5 min, chilled on ice, and then applied to a 20% denaturing polyacrylamide gel. The gel was run at 45 W for 2.5 h and then visualized by autoradiography and storage phosphor autoradiography.

Fe^{II}·BLM Cleavage of the DNA Triplex. Reaction mixtures (20 μL total volume) contained 10 nM duplex (1×10^5 cpm) and 10 μM 11-mer in 10 mM sodium cacodylate (pH 6.0) containing 100 mM NaCl and 2.5 or 5 μM Fe^{II}·BLM A_2. Reaction mixtures were incubated for 1 h at 0 °C, and then the reactions were quenched with EDTA (to a final concentration of 5 mM) and 5 μL of gel loading solution. Samples were heated at 90 °C for 5 min, chilled on ice and then applied to a 20% denaturing polyacrylamide gel. The gel was run at 45 W for 2.5 h and then visualized by autoradiography and storage phosphor autoradiography.

Fe^{II}·MPE Degradation of the 32 bp Duplex. The complementary 32-mer oligodeoxynucleotides were hybridized in 10 μL (total volume) of 10 mM Tris-HCl (pH 7.4) containing 100 mM NaCl, 0.5 μM unlabeled strand, and 0.4 μM ^{32}P-labeled strand (2.5×10^6 cpm). The solution was heated at 90 °C for 2 min and then allowed to cool to room temperature over a period of 1 h. Reaction mixtures (20 μL total volume) contained 10 nM duplex (1×10^5 cpm) and 20 μM (nt concentration) carrier calf thymus DNA in 10 mM Tris-HCl (pH 7.4) with 50 mM NaCl and 5 μM Fe^{II}·MPE. The cleavage reaction was initiated by the addition of DTT to a 1 mM final concentration. The reaction mixtures were incubated for 30 min at room temperature, and then the reactions were quenched with 1 μg of calf thymus DNA, EDTA (to a final concentration of 5 mM), and 10 μL of loading solution. Samples were heated at 90 °C for 5 min, chilled on ice, and then applied to a 20% denaturing polyacrylamide gel. The gel was run at 45 W for 2.5 h and then visualized by autoradiography and storage phosphor autoradiography.

Molecular Modeling. Molecular modeling by conformational energy minimization was carried out using the JUMNA program package (version IV) (Lavery, 1988). Neither water nor positively charged counterions were explicitly included in the calculations. However, their effects were mimicked by a sigmoidal, distance-dependent, dielectric function (Hingerty et al., 1985; Lavery, 1988) and by assignment of a half-charge for each phosphate group. No cutoff distances were used. Computations were performed on a Silicon Graphics 4D/120GTXB dual processor workstation.

The coordinates of triples helices were derived from the previously published B-like triple helices (Ouali et al., 1993) which is now widely supported by numerous NMR and vibrational spectroscopic studies. The calculation procedure was similar to that reported in the previous study on the double−triple helix junction (Chomilier et al., 1992). The structural properties of triple helices were analyzed using the CURVE algorithm (Lavery & Sklenar, 1989) which calculates a full set of independent helicoidal coordinates and an optimal global axis for nucleic segments with up to four strands. Groove widths were measured at the level of the base triplets as the minimal distance between spline-fitted curves passing through the phosphorus atoms of each backbone (less 5.8 Å, representing the van der Waals radii of the phosphate groups). Groove depths were then calculated as the distance between the minimal length vector joining the backbones and the appropriate face of the base triplet (Stofer & Lavery, 1993).

RESULTS

[$Phen_2$·Cu^I]$^+$ Footprinting and Fe^{II}·BLM-Mediated Cleavage of the DNA Triple Helix. The formation of a triple helix and its subsequent cleavage by Fe^{II}·BLM is illustrated in Figure 3. The pyrimidine-rich strand was 5′-^{32}P end-labeled, and the sequence was verified by chemical sequencing analysis (lanes 4−7). Cu^{II}·(phenanthroline)$_2$ ([$Phen_2$·Cu^I]$^+$) cleavage was used to demonstrate the formation of the triplex under the conditions employed. DNA cleavage by [$Phen_2$·Cu^I]$^+$ is sensitive to local variations in DNA conformation. The products of [$Phen_2$·Cu^I]$^+$-mediated DNA strand scission, oligonucleotides terminating in 3′-phosphate (major) and 3′-phosphoroglycolate groups (minor), are consistent with attack of the reactive species from the minor groove (Sigman, 1986). As is clear from lanes 1 and 2, in the presence of the oligopyrimidine 11-mer protection from cleavage was observed in a well-defined region of the DNA strand, providing a detailed "footprint" of the triplex region and providing unequivocal evidence that the triplex was formed under the reaction conditions. In addition, increased cleavage was observed at the duplex−triplex junction on the 5′-side of the 11-mer third strand, as observed previously (François et al., 1988).

The ability of Fe^{II}·BLM to cleave the pyrimidine-rich strand of the DNA triplex selectively at 2.5 μM (lanes 8 and 9) and 5 μM concentrations (lanes 10 and 11) was demonstrated. At 2.5 μM Fe^{II}·BLM, cleavage of the duplex was not observed, although significant degradation of the triplex was observed. Lanes 10 and 11 illustrate cleavage

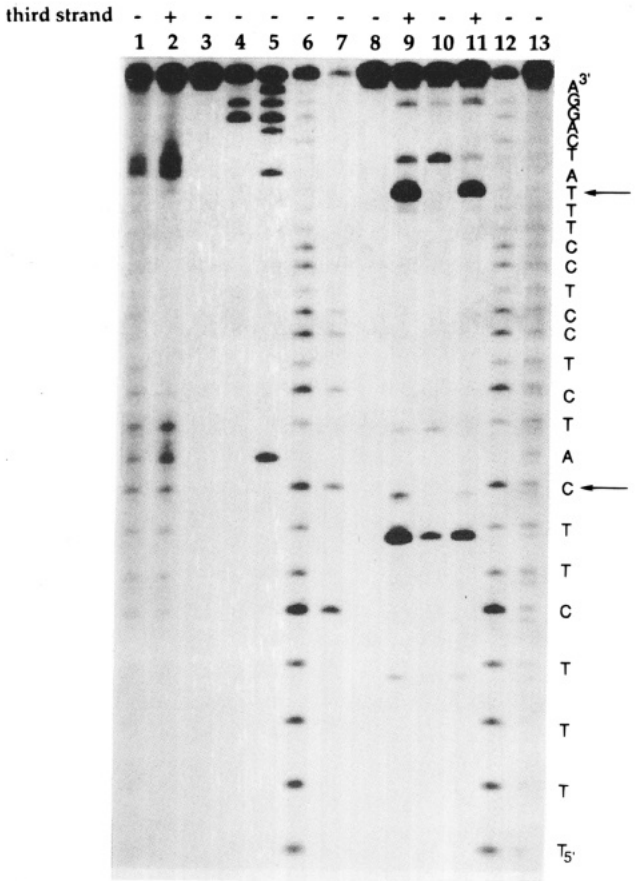

FIGURE 3: Autoradiogram of a 20% polyacrylamide gel illustrating $[Phen_2 \cdot Cu^I]^+$ footprinting and Fe^{II}·BLM cleavage of the pyrimidine-rich strand of the DNA triple helix. The pyrimidine-rich strand was 5′-^{32}P end-labeled. Lanes 2, 9, and 11 contained the 11-mer homopyrimidine oligonucleotide in addition to the duplex. The arrows indicate the unique triplex cleavage sites: lanes 1 and 2, 15 μM $[Phen_2 \cdot Cu^I]^+$; lane 3, duplex alone; lane 4, G lane; lane 5, G+A lane; lane 6, C+T lane; lane 7, C lane; lanes 8 and 9, 2.5 μM Fe^{II}·BLM A_2; lanes 10 and 11, 5 μM Fe^{II}·BLM A_2; lane 12, C+T lane; lane 13, 5 μM Fe^{II}·MPE.

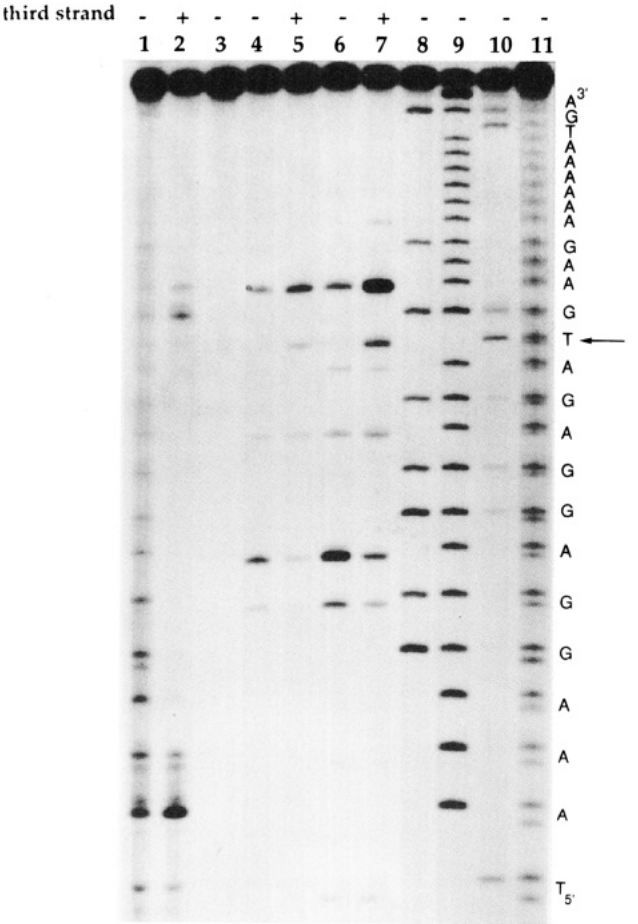

FIGURE 4: Autoradiogram of a 20% polyacrylamide gel demonstrating $[Phen_2 \cdot Cu^I]^+$ footprinting and Fe^{II}·BLM cleavage of the purine-rich strand of the DNA triplex. The purine-rich strand was 5′-^{32}P end-labeled. Lanes 2, 5, and 7 contained the 11-mer homopyrimidine oligonucleotide in addition to the duplex. The arrow indicates the unique triplex cleavage site: lanes 1 and 2, 15 μM $[Phen_2 \cdot Cu^I]^+$; lane 3, duplex alone; lanes 4 and 5, 2.5 μM Fe^{II}·BLM A_2; lanes 6 and 7, 5 μM Fe^{II}·BLM A_2; lane 8, G lane; lane 9, G+A lane; lane 10, C+T lane; lane 11, 5 μM Fe^{II}·MPE.

by 5 μM Fe^{II}·BLM of the duplex and triplex, respectively. A few observations can be made, namely (i) several cleavage sites were common to both substrates, (ii) two cleavage sites were unique to the triplex and were more pronounced at the lower drug concentration, and (iii) changes in the intensities of the common cleavage sites were observed in the presence of the 11-mer homopyrimidine oligonucleotide. The cleavage site closest to the 3′-end of the pyrimidine-rich strand involved thymidine$_8$ at the 5′-duplex−triplex junction (note that the 5′ → 3′ directionality of the triplex is considered the same as that of the 11-mer pyrimidine oligonucleotide; all strands are numbered from the left as shown). The second cleavage site on this strand unique to the triplex was at cytidine$_{20}$, located two nucleotides from the 3′-duplex−triplex junction. This band was more pronounced at 2.5 μM Fe^{II}·BLM than at 5 μM Fe^{II}·BLM.

To determine the chemical nature of the 3′-termini of the cleavage fragments, the DNA duplex was digested with Fe^{II}·methidium propyl−EDTA (MPE) to provide authentic standards for comparison with the triplex cleavage products. The products of Fe^{II}·MPE-mediated DNA degradation consist of a mixture of fragments terminating in 3′-phosphates and 3′-phosphoroglycolates at each position, which migrate as two closely spaced bands on polyacrylamide gels (Henner et al., 1983; Hertzberg & Dervan, 1984). The 3′-phosphoroglycolate product has been shown to be the faster migrating product. It was quite clear that the cleavage fragments produced by Fe^{II}·BLM terminated in 3′-phosphoroglycolates, as well as lesser amounts of fragments which terminated in 3′-phosphates. To identify the 3′-termini of the cleavage products close to the 3′-end of the strand, electrophoresis was carried out for an increased length of time to obtain better resolution; these cleavage fragments also terminated in 3′-phosphoroglycolates, including the triplex-specific cleavage fragment (data not shown).

Shown in Figure 4 is the cleavage of the 5′-^{32}P end-labeled purine-rich strand by Fe^{II}·BLM. The sequence was verified by chemical-sequencing analysis (lanes 8−10). $[Phen_2 \cdot Cu^I]^+$ footprinting was carried out in lanes 1 and 2. A defined region of protection was observed in the presence of the 11-mer homopyrimidine oligonucleotide. The homopurine tract located near the 3′-terminus was cleaved very weakly by the $[Phen_2 \cdot Cu^I]^+$ complex, analogous to results published previously (François et al., 1988). Lanes 4−7 illustrate Fe^{II}·BLM-mediated cleavage of the duplex and triplex at 2.5 and 5 μM Fe^{II}·BLM. In common with the pyrimidine strand, several cleavage sites were observed for the purine strand of both the duplex and triplex; the intensities of the common cleavage sites varied from one substrate to the other. In

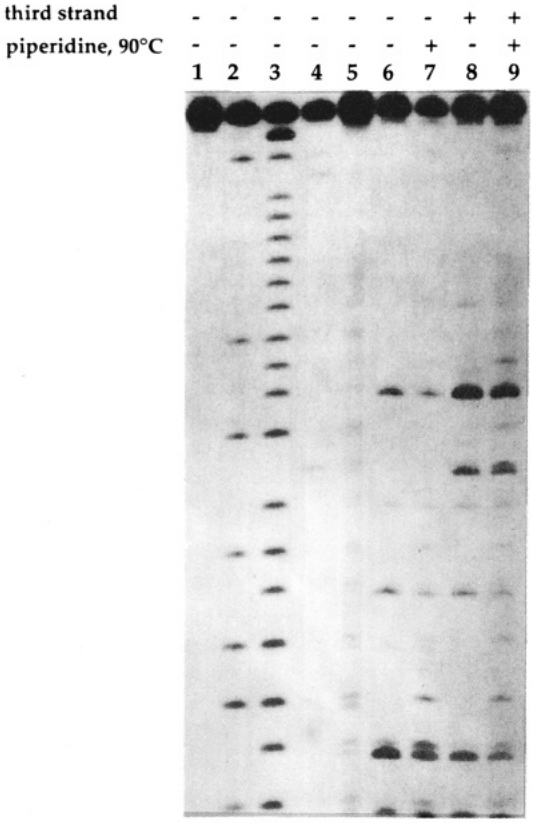

FIGURE 5: Autoradiogram of a 20% polyacrylamide gel demonstrating piperidine-induced cleavage of the DNA triplex alkali labile lesions. The purine-rich strand was 5′-^{32}P end-labeled. Lanes 8 and 9 contained the 11-mer homopyrimidine oligonucleotide in addition to the duplex: lane 1, duplex alone; lane 2, G lane; lane 3, G+A lane; lane 4, C+T lane; lane 5, 5 μM Fe^{II}·MPE; lane 6, 5 μM Fe^{II}·BLM A_2; lane 7, 5 μM Fe^{II}·BLM A_2, followed by incubation with piperidine at 90 °C; lane 8, 5 μM Fe^{II}·BLM A_2; lane 9, 5 μM Fe^{II}·BLM A_2, followed by incubation with piperidine at 90 °C.

contrast to observations for the pyrimidine strand, cleavage of the purine strand of the duplex was observed at both 2.5 and 5 μM Fe^{II}·BLM, but only one unique triplex site was observed adjacent to the 3′-duplex−triplex junction at thymidine$_{19}$. Comparison of the cleavage fragments produced by Fe^{II}·BLM with those produced by Fe^{II}·MPE (lane 11) demonstrated that the products of BLM-mediated cleavage of the purine-rich strand of the triplex terminated in 3′-phosphoroglycolates, including the triplex-specific cleavage fragment.

Bleomycin-mediated DNA degradation can occur by two pathways. One of these results directly in DNA strand scission, producing fragments terminating in 3′-phosphoroglycolates and releasing base propenals; the other affords alkali labile lesions with the concomitant release of free bases (Hecht, 1986; Stubbe & Kozarich, 1987; Natrajan & Hecht, 1993; Kane & Hecht, 1994). Base treatment of the alkali labile sites results in DNA strand scission, producing fragments terminating in 3′-phosphates (Sugiyama et al., 1985b, 1988; Rabow et al., 1986). To reveal any alkali labile sites on the DNA triplex following incubation with Fe^{II}·BLM, reaction mixtures were treated with piperidine at 90 °C. Figure 5 demonstrates that two products were formed during Fe^{II}·BLM-mediated degradation of the triplex (the purine-rich strand is shown). Doublet bands were observed at all sites, and the intensities of the 3′-phosphate bands increased substantially after treatment with piperidine. The same products were observed for degradation of the pyrimidine-rich strand (data not shown).

Cleavage of the DNA Triple Helix by Fe^{II}·Phleomycin. The fact that the strongest cleavage site induced by Fe(II)·BLM occurred at the 5′-duplex−triplex junction was of particular interest because the 5′-junction has been determined to be the preferred triple helix binding site of certain intercalating agents (Perrouault et al., 1990; Collier et al., 1991a). The preference of BLM for the 5′-junction was intriguing because, while there is evidence suggesting that BLM may bind to B-form DNA by a (partial) intercalative mechanism (Chien et al., 1977; Povirk et al., 1979; Levy & Hecht, 1988; Wu et al., 1994; Manderville et al., 1995), there is overwhelming evidence that the binding of BLM to DNA involves minor groove interactions (Sugiura & Suzuki, 1982; Suzuki et al., 1983; Hertzberg et al., 1988; Kuwahara & Sugiura, 1988; Manderville et al., 1994, 1995). In order to determine whether the preference of BLM for the 5′-junction reflected an intercalative mode of association with the DNA triplex, the selectivity of cleavage of the triplex by Fe^{II}·BLM was compared with the selectivity exhibited by Fe^{II}·phleomycin (PLM) (cf. Figure 1). PLM contains a thiazolinylthiazole ring system rather than a planar bithiazole and should be incapable of intercalation; in fact, it has been shown not to bind to DNA via intercalation (Povirk et al., 1981). However, PLM exhibits $^{5'}$G-Pyr$^{3'}$ selectivity of cleavage of duplex DNA very similar to that of BLM (Kross et al., 1982). Shown in Figure 6 is the cleavage of the 5′-^{32}P end-labeled pyrimidine-rich strand of the DNA triplex by both BLM and PLM. The specificity of both BLM and PLM for cleavage at the 5′-junction was immediately apparent (compare lanes 3 and 5 and 7 and 9). The selectivity of strand scission by both compounds was quite similar, although variations in the intensities of some of the cleavage bands were observed. Additionally, both BLM and PLM mediated triplex-specific cleavage near the 3′-junction. A similar selectivity of cleavage of the purine-rich strand of the triplex was observed for BLM and PLM (Figure 7), with triplex-specific cleavage at the 3′-junction. The unique triple helix cleavage sites induced by BLM and PLM are summarized in Figure 8 at 2.5 μM concentrations of each compound. Very similar results were obtained at 5 μM concentrations of each. Both compounds mediated triplex-specific cleavage at the same unique sites near the duplex−triplex junctions. Moreover, PLM mediated cleavage at the 5′-junction with even greater selectivity than BLM. These results provided strong evidence that the cleavage specificity of Fe^{II}·BLM for the 5′-junction was not related to a selective intercalative mode of association with the triple helical structure.

Further, the fact that BLM and PLM exhibit quite similar effects in binding both to B-form DNA (Kross et al., 1982) and to the duplex−triplex junction studied here reinforces the idea that both may bind to DNA in the same fashion. Since PLM should be incapable of binding to DNA by intercalation (Povirk et al., 1981), it seems likely that the binding observed in analogous situations for bleomycin also obtains without classical intercalation of the bithiazole moiety.

Structural Alterations Induced upon Triple Helix Formation. Molecular-modeling calculations of the triple helix region have been carried out using coordinates obtained for the triplex base sequences poly(T·A_xT), poly(C·$G_x$$C^+$), and alternating poly(T·A_xT)/poly(C·$G_x$$C^+$) (Ouali et al., 1993)

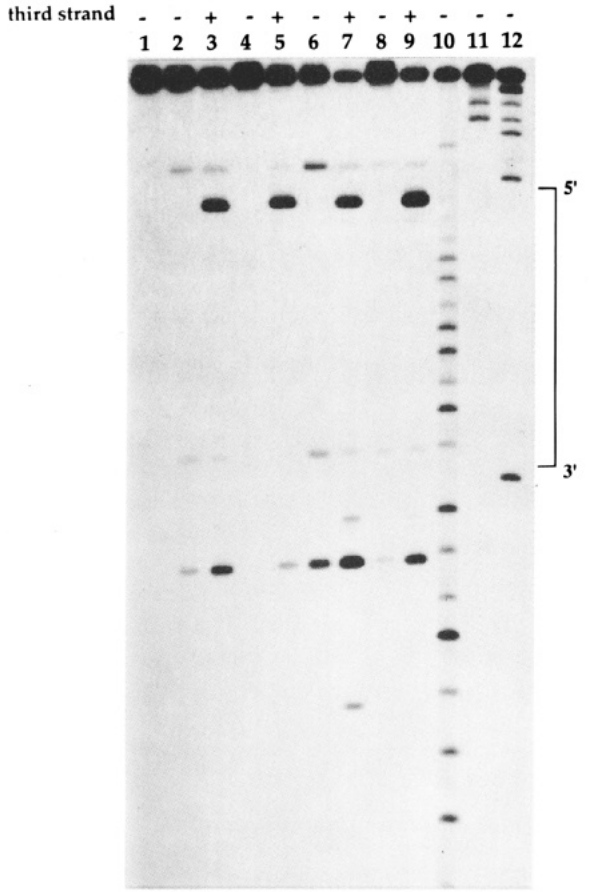

FIGURE 6: Autoradiogram of a 20% polyacrylamide gel illustrating cleavage of the DNA triplex by Fe^{II}·BLM and Fe^{II}·PLM. The pyrimidine-rich strand was 5′-^{32}P end-labeled. Reaction mixtures containing Fe^{II}·PLM were run in a manner analogous to that of the Fe^{II}·BLM reactions. Lanes 3, 5, 7, and 9 contained the 11-mer homopyrimidine oligonucleotide in addition to the duplex: lane 1, duplex DNA alone; lanes 2 and 3, 2.5 μM Fe^{II}·BLM A_2; lanes 4 and 5, 2.5 μM Fe^{II}·PLM; lanes 6 and 7, 5 μM Fe^{II}·BLM A_2; lanes 8 and 9, 5 μM Fe^{II}·PLM; lane 10, C+T lane; lane 11, G lane; lane 12, G+A lane.

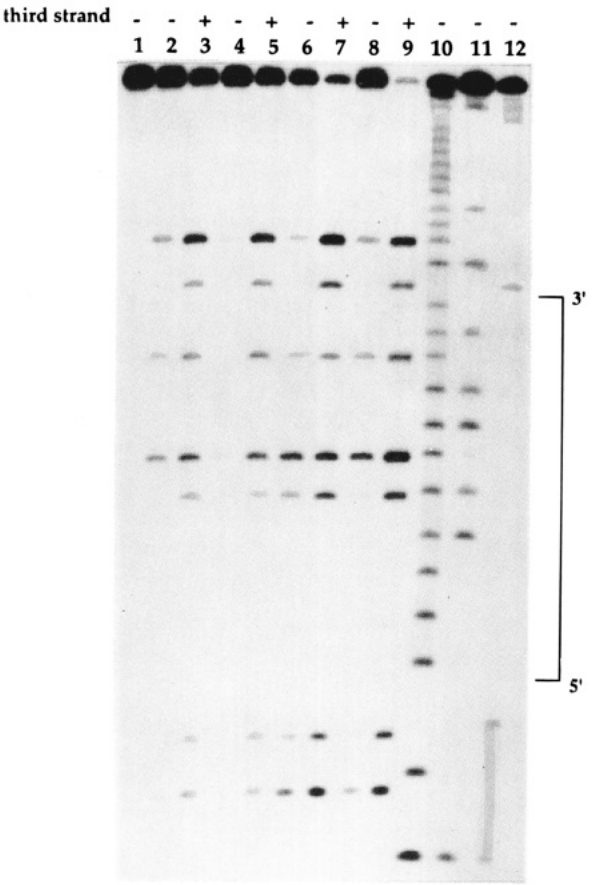

FIGURE 7: Autoradiogram of a 20% polyacrylamide gel demonstrating cleavage of the DNA triplex by Fe^{II}·BLM and Fe^{II}·PLM. The purine-rich strand was 5′-^{32}P end-labeled. Reaction mixtures containing Fe^{II}·PLM were run in a manner analogous to that of the Fe^{II}·BLM reactions. Lanes 3, 5, 7, and 9 contained the 11-mer homopyrimidine oligonucleotide in addition to the duplex: lane 1, duplex alone; lanes 2 and 3, 2.5 μM Fe^{II}·BLM A_2; lanes 4 and 5, 2.5 μM Fe^{II}·PLM; lanes 6 and 7, 5 μM Fe^{II}·BLM A_2; lanes 8 and 9, 5 μM Fe^{II}·PLM; lane 10, G+A lane; lane 11, G lane; lane 12, C+T lane.

in order to study the conformational changes in the minor groove induced upon triple helix formation; these data are presented in Figure 9. The minor groove of the triplex was calculated to be somewhat shallower and wider than the minor groove of the corresponding duplex but did not approach the dimensions of an A-form duplex [which exhibits dimensions of 11 and 2.7 Å for the width and depth, respectively (Saenger, 1984)]. Dramatic changes in the dimensions of the minor groove were observed at the duplex−triplex junctions (nucleotide positions 6 and 16), particularly at the 5′-junction, where the minor groove width increased from 3.6 to 6.4 Å within three nucleotides. Interestingly, the variations observed for the minor groove width and depth were asymmetric with regard to the 5′- and 3′-junctions. Additionally, all sugars exhibited C-2′-endo sugar puckering, with the exceptions of cytidine$_{18}$ in the pyrimidine strand and adenosine$_7$ in the purine strand, which exhibited O-1′-endo sugar puckering. Comparison of these data to the unique cleavage sites induced by Fe^{II}·BLM demonstrated that the BLM cleavage sites corresponded to the regions where the dimensions of the minor groove width and depth displayed dramatic variations, particularly at the 5′-junction.

Storage phosphor densitometry of the polyacrylamide gels shown in Figures 3 and 4 was carried out to obtain additional information regarding the differences between the duplex and triplex structures. A summary of all BLM cleavage sites, in both the duplex and triplex, as well as the relative intensity of cleavage at each site, is illustrated in Figure 10 for 5 μM Fe^{II}·BLM A_2. The comparable data for 2.5 μM Fe^{II}·BLM A_2 are given in the supporting information. Several observations can be made. The intensities of the cleavage sites on each strand varied from duplex to triplex. Interestingly, some cleavage sites were enhanced in the presence of the third strand (in addition to those sites unique to the triplex), while some were suppressed. In addition, only the purine-rich strand was cleaved within the triple helix region (the pyrimidine-rich strand was cleaved only at the duplex−triplex junctions). Moreover, most of these sites were decreased in intensity in the presence of the third strand. Finally, minimal cleavage was observed within the tract of six adenosines located near the 3′-end of the triplex.

Effect of Mg^{2+} on Fe^{II}·BLM-Mediated Cleavage of the Triplex. The effect of added Mg^{2+} on the cleavage of the DNA triplex by Fe^{II}·BLM was examined. Divalent metal ions are known to stabilize nucleic acid structures (Saenger, 1984). Moreover, Mg^{2+} has been shown to alter the facility with which Fe^{II}·BLM mediates RNA cleavage (Hüttenhofer et al., 1992; Holmes et al., 1993), although it has been shown to have little effect on B-form DNA cleavage

FIGURE 8: Sites of triplex-specific cleavage mediated by Fe^{II}•BLM and Fe^{II}•PLM. The relative intensities of cleavage were determined by storage phosphor densitometry of the polyacrylamide gels in Figures 6 (lanes 3 and 5) and 7 (lanes 3 and 5). The cleavage intensities were corrected for the total amount of radiolabeled DNA in that lane.

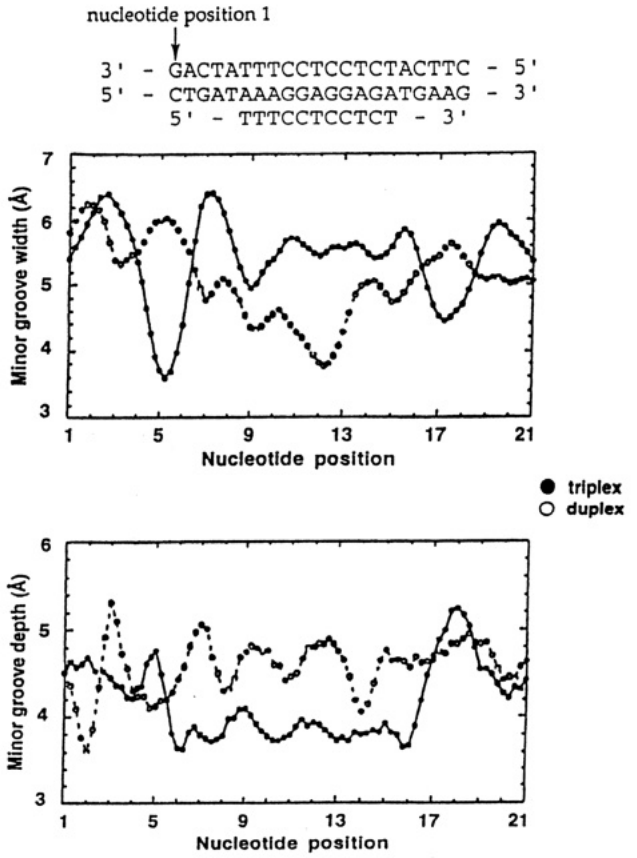

FIGURE 9: Molecular-modeling calculations of the variation of the minor groove width and depth upon triple helix formation.

by BLM (Hertzberg et al., 1988). Cleavage of the triplex was carried out in the presence of 0, 0.5, 1, 2, or 5 mM $MgCl_2$, and the extent of cleavage at the unique triplex cleavage sites was determined by storage phosphor densitometry. As shown in Table 1, concentrations of Mg^{2+} up to 5 mM had little, if any, effect on the cleavage of the triple helix by Fe^{II}•BLM. In fact, as the concentration of Mg^{2+} increased to 2 mM, a slight enhancement in the extent of cleavage of the pyrimidine-rich strand was observed. Importantly, no change in the sites of cleavage on either strand was observed in the presence of Mg^{2+}. Moreover, the concentration of Mg^{2+} affected the extent of cleavage proportionately at *all* cleavage sites (data not shown).

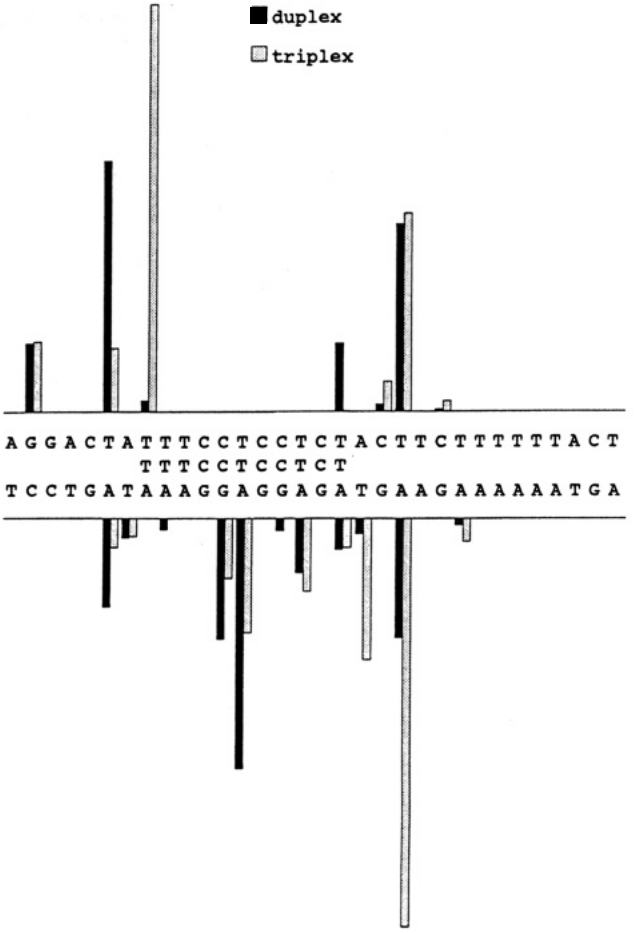

FIGURE 10: Summary of the cleavage sites induced by 5 μM Fe^{II}•BLM A_2 within the duplex and triplex. Storage phosphor densitometry of the polyacrylamide gels in Figures 3 (lanes 10 and 11) and 4 (lanes 6 and 7). The intensity of cleavage at each site was normalized for the total amount of radiolabeled DNA in that lane.

Table 1: Effect of Mg^{2+} on Fe^{II}•BLM-Mediated Cleavage of the Triple Helix[a]

Mg^{2+} concentration (μM)	% cleavage	
	pyrimidine-rich strand	purine-rich strand
0	16	6
0.5	17	10
1	22	5
2	22	5
5	14	6

[a] Reaction mixtures contained 5 μM Fe^{II}•BLM A_2 and the indicated concentration of Mg^{2+}. Cleavage of the pyrimidine strand refers to the intensity of cleavage at T_8; cleavage of the purine strand refers to the intensity of cleavage at T_{19} (cf. Figure 2 for numbering). The relative intensities of cleavage were determined by storage phosphor densitometry. The cleavage intensities were corrected for the total amount of radiolabeled DNA in that lane.

DISCUSSION

The initial observation that poly(U) and poly(A) form a stable 2:1 triple helix was made almost four decades ago (Felsenfeld et al., 1957). Since that observation, the structure and sequence requirements for the formation of triple helices have been investigated in great detail (Thuong & Hélène, 1993). There has been renewed interest in these types of nucleic acid structures in recent years due to their potential therapeutic applications. Short oligonucleotides can specifically recognize double-stranded DNA sequences from the major groove side (Le Doan et al., 1987; Moser & Dervan, 1987). Triple helical complexes may inhibit gene transcription in a gene-specific manner (Cooney et al., 1988; Grigoriev et al., 1992, 1993). Intramolecular triple helices, or H-DNA, appear to be involved in gene regulation and recombination (Htun & Dahlberg, 1988; Johnson, 1988). Triple helix formation has been used to impart sequence specificity to DNA-cleaving agents and intercalating agents (Le Doan et al., 1987; Moser & Dervan, 1987; François et al., 1989b; Sun et al., 1989; Perrouault et al., 1990). In addition, the binding of a third strand to double-stranded DNA has been shown to inhibit DNA binding proteins (François et al., 1989b; Maher et al., 1989; Collier et al., 1991b). Recently, this approach has been used to mediate the cleavage of human chromosomal DNA at a single site (Strobel et al., 1991). These findings suggest the utility of oligonucleotide-directed triple helix formation in the modulation of gene expression and alteration of the site(s) of enzyme activity. Further, oligonucleotides coupled to DNA-cleaving agents may prove to be powerful tools for gene analysis and chromosome mapping. In the present case, triple helix formation was used to alter the usual selectivity of a clinically important DNA-cleaving agent, thereby creating a unique, highly specific target for cleavage.

Initial studies focused on footprinting of the triple helix region, to insure that the triplex was indeed formed under the experimental conditions used in this study. As illustrated in Figures 3 and 4, binding of the homopyrimidine oligonucleotide to the 32 bp duplex afforded protection from attack by $[Phen_2 \cdot Cu^I]^+$. $[Phen_2 \cdot Cu^I]^+$ has been shown to attack via the minor groove (Sigman, 1986). The inhibition of cleavage within the triple helix region by $[Phen_2 \cdot Cu^I]^+$ was remarkable, because it has been shown that the binding of *Eco*RI endonuclease in the major groove of the dodecamer d(GCGCAATTCGCG) did not protect against cleavage by the coordination complex (Kuwabara et al., 1986). Therefore, the region of protection afforded by the pyrimidine oligonucleotide against cleavage by $[Phen_2 \cdot Cu^I]^+$ most likely reflects a structural change in the minor groove induced upon the binding of the oligonucleotide in the major groove.

After it was shown that the triplex is formed under the experimental conditions employed, the ability of $Fe^{II} \cdot$BLM to degrade the triplex was investigated. As shown in Figures 3 and 4, incubation of the 32 bp duplex and the 11-mer pyrimidine oligonucleotide with 2.5 or 5 μM $Fe^{II} \cdot$BLM resulted in specific cleavage of the DNA triplex. Cleavage sites were observed on both strands, at the duplex−triplex junctions (Figure 8). The primary products of cleavage were oligonucleotides terminating in 3′-phosphoroglycolates, as determined by comparison with the products resulting from cleavage by $Fe^{II} \cdot$MPE. These products are analogous to those produced upon cleavage of double-stranded DNA by $Fe^{II} \cdot$BLM. Since $Fe^{II} \cdot$BLM-mediated degradation of duplex DNA can proceed by two pathways (Hecht, 1986; Stubbe & Kozarich, 1987; Natrajan & Hecht, 1993; Kane & Hecht, 1994), one resulting directly in strand scission and another that affords alkali labile lesions, the possible formation of alkali labile sites within the triplex structure was investigated. Following incubation with $Fe^{II} \cdot$BLM, the DNA was incubated with piperidine at 90 °C (Figure 5). Incubation of the BLM-treated DNA with piperidine resulted in DNA strand scission, producing cleavage fragments terminating in 3′-phosphate groups. BLM-mediated degradation of the triplex therefore resulted in direct strand scission, as well as the formation of alkali labile lesions. These results provided strong evidence that the mechanism of BLM-mediated degradation of the triple helix was analogous to the cleavage of a B-form DNA duplex by the drug. Abstraction of the C-4′ H presumably resulted in the formation of a transient C-4′ deoxyribose radical which partitioned between two pathways, leading to two sets of products (Hecht, 1986; Stubbe & Kozarich, 1987; Natrajan & Hecht, 1993; Kane & Hecht, 1994).

The available evidence suggests that BLM may bind to DNA through (partial) intercalation (Chien et al., 1977; Povirk et al., 1979; Hénichart et al., 1985; Levy & Hecht, 1988; Wu et al., 1994; Manderville et al., 1995). However, additional observations strongly suggest that BLM binding to DNA involves minor groove contacts. These include altered selectivity of cleavage in the presence of the minor groove binder distamycin (Sugiura & Suzuki, 1982; Sugiyama et al., 1985a) and inhibition of cleavage at $^{5'}GC^{3'}$ and $^{5'}GT^{3'}$ sequences of DNA which had been modified in the minor groove by anthramycin (Kuwahara & Sugiura, 1988). Recent NMR studies using $Zn^{II} \cdot$BLM and a synthetic DNA duplex provide compelling evidence for extensive BLM−DNA contacts within the minor groove (Manderville et al., 1994, 1995). The fact that cleavage is initiated by abstraction of the C-4′ H (Wu et al., 1983, 1985; Kozarich et al., 1989) also supports the minor groove binding model. In order to determine whether the preference of BLM for the 5′-junction reflected intercalative binding at the junction, the selectivity of cleavage by BLM was compared with the selectivity of PLM. As demonstrated in Figures 6 and 7, BLM and PLM mediated triplex-specific cleavage at the same sites. The relative intensities of cleavage are summarized in Figure 8. Interestingly, PLM, which is unable to intercalate into DNA, exhibited an even greater selectivity for the 5′-junction than BLM. Further, while PLM has been noted to cleave B-DNA with somewhat less efficiency than BLM (Kross et al., 1982), as reflected in Figures 6 and 7, the two agents cleaved the DNA triple helix with comparable efficiencies. These results provided strong evidence that the cleavage specificity of $Fe^{II} \cdot$BLM for the 5′-junction was not related to an intercalative mode of binding at the junction, but rather to recognition of a minor groove shape inherent to the duplex−triplex junctions.

There is a dearth of information regarding the structures of triple helices. The only DNA triple helix structure described in detail is that of fibers of poly(dA)·2poly(dT) (Arnott & Selsing, 1974). X-ray diffraction patterns suggested an A-form, RNA-like structure with a presumed C-3′-endo sugar pucker. For many years, this was the accepted model and formed the basis for most investigations of triple helix structures. More recently, infrared spectral studies of

poly(dA)·2poly(dT) have suggested that the structure adopts a B-form geometry, with a C-2′-endo sugar pucker (Howard et al., 1992). Interestingly, the minor groove binding drugs distamycin and netropsin, which bind preferentially to B-form DNA, have been shown to bind to DNA triple helices (Howard et al., 1992; Park & Breslauer, 1992) without inducing the expulsion of the third strand. However, netropsin was shown to bind to the triplex at a lower saturation binding density than to the duplex, suggesting that the binding of an oligonucleotide in the major groove of duplex DNA induces a conformational change in the minor groove. ^{1}H NMR data have shown that, in DNA triple helices, the pyrimidine strands contained a mixture of C-3′ and C-2′-endo sugar puckers, while the purine strand was overwhelmingly C-2′-endo (Macaya et al., 1992a,b), suggesting that the triplex structure was more heterogeneous than a DNA duplex. Moreover, a recent study using molecular-modeling calculations in combination with vibrational spectroscopy demonstrated that triple helices containing C-2′-endo sugar puckers were both stereochemically and energetically feasible and were consistent with recent spectroscopic studies (Ouali et al., 1993). Molecular-modeling calculations of the triple helix region of the sequence employed in our investigation support the current models of triplex structure which suggest strongly that DNA triple helices more closely resemble B-DNA than an A-form helix, although the minor groove was calculated to be somewhat wider and shallower than the minor groove of a B-form DNA helix. In this context, it may be noted that the fact that Mg^{2+} had no effect on the cleavage of the triplex by BLM supports the idea that the triplex structure is more DNA-like than RNA-like. Cleavage of duplex DNA by BLM is largely unaffected by $MgCl_2$, except at very high concentrations (Hertzberg et al., 1988). On the other hand, RNA cleavage by BLM can be highly sensitive to Mg^{2+} and other reagents that affect RNA structure (Hüttenhofer et al., 1992; Holmes et al., 1993).

Additional insight regarding the differences between the duplex and triplex structures was gained from these experiments. The sites of cleavage induced by Fe^{II}·BLM for both the duplex and triplex, as well as the relative intensities of cleavage at each site, are summarized in Figure 10. For the cleavage sites that were common to both substrates, the intensities of cleavage were different in the presence of the homopyrimidine oligonucleotide. Interestingly, some of these cleavage sites were enhanced in the presence of the third strand while others were suppressed. These observations support the molecular-modeling data and published results (*vide supra*) which indicate that significant changes in local DNA conformation accompany triple helix formation. These changes led to a change in the selectivity of cleavage by Fe^{II}·BLM. Within the core region of the triplex, only the purine-rich strand was cleaved (the pyrimidine-rich strand was cleaved only at the duplex−triplex junctions). Moreover, most of these sites were suppressed in the presence of the third strand. Finally, minimal cleavage was observed within the tract of six adenosines located near the 3′-end of the triplex. The minor groove of sequences containing A·T base pairs is deeper than that of sequences containing G·C base pairs, due to the absence of the 2-amino group of guanosine. Moreover, it has been shown that the minor groove of some A+T-rich sequences is narrower than that of typical B-DNA (Yoon et al., 1988). These observations support the idea that nucleic acid sequences exhibiting a wider and shallower minor groove, such as the $^{5'}$GC$^{3'}$ sequences in B-DNA and the sequences found in RNA and DNA triple helices, are actually the source of nucleic acid recognition by Fe^{II}·BLM. Although the present data do not permit the orientation of Fe^{II}·BLM on the DNA triple helix to be deduced, the dramatic changes in minor groove width and depth at the duplex−triplex junctions within a few nucleotides of the sites of cleavage would clearly permit the binding of BLM to a groove of optimal shape in proximity to the sites of cleavage.

CONCLUSIONS

The highly specific cleavage of a DNA triple helix by Fe^{II}·BLM has been demonstrated. The most intense cleavage site was at the 5′-junction on the pyrimidine-rich strand. Cleavage also occurred on both strands at the 3′-junction. Strand scission products and alkali labile lesions were formed. The products of cleavage of the triplex by Fe^{II}·BLM were the same as those formed from cleavage of duplex DNA, implying that the mechanism of cleavage of the triplex was analogous to that of cleavage of duplex DNA, i.e., involving initial H abstraction from C-4′ of deoxyribose. The specificity of Fe^{II}·BLM for the 5′-junction appeared to derive from recognition of a minor groove shape within this sequence, as opposed to intercalation at the junction. This is supported by the observation that Fe^{II}·PLM, which is structurally incapable of binding to DNA by intercalation, exhibited the same selectivity of triplex cleavage as Fe^{II}·BLM. The finding that cleavage of the DNA triplex occurred in the presence of Mg^{2+} concentrations up to 5 mM is consistent with the potential therapeutic relevance of triplexes as targets for Fe^{II}·BLM. This study has revealed a novel polynucleotide target for Fe^{II}·BLM; the selectivity of cleavage clearly reflected recognition of unusual DNA conformations by Fe^{II}·BLM. The ability to alter the usual selectivity of a DNA-cleaving agent and to create unique, highly specific targets for cleavage represents a new application for the technology of oligonucleotide-directed triple helix formation.

SUPPORTING INFORMATION AVAILABLE

Summary of the intensity of cleavage induced by 2.5 μM BLM A_2 at specific sites within the duplex and triplex (1 page). Ordering information is given on any current masthead page.

REFERENCES

Arnott, S., & Selsing, E. (1974) *J. Mol. Biol. 88*, 509−521.
Burger, R. M., Peisach, J., & Horwitz, S. B. (1981) *J. Biol. Chem. 256*, 11636−11644.
Carter, B. J., deVroom, E., Long, E. C., van der Marel, G. A., van Boom, J. H., & Hecht, S. M. (1990) *Proc. Natl. Acad. Sci. U.S.A. 87*, 9373−9377.
Caruthers, M. H. (1985) *Science 230*, 281−285.
Chien, M., Grollman, A. P., & Horwitz, S. B. (1977) *Biochemistry 16*, 3641−3647.
Chomilier, J., Sun, J.-S., Collier, D. A., Garestier, T., Hélène, C., & Lavery, R. (1992) *Biophys. Chem. 45*, 143−152.
Collier, D. A., Mergny, J.-L., Thuong, N. T., & Hélène, C. (1991a) *Nucleic Acids Res. 19*, 4219−4224.
Collier, D. A., Thuong, N. T., & Hélène, C. (1991b) *J. Am. Chem. Soc. 113*, 1457−1458.
Cooney, M., Czernuszewicz, G., Postel, E. H., Flint, S. J., & Hogan, M. E. (1988) *Science 241*, 456−459.
D'Andrea, A. D., & Haseltine, W. A. (1978) *Proc. Natl. Acad. Sci. U.S.A. 75*, 3608−3612.

Ehrenfeld, G. M., Shipley, J. B., Heimbrook, D. C., Sugiyama, H., Long, E. C., van Boom, J. H., van der Marel, G. A., Oppenheimer, N. J., & Hecht, S. M. (1987) *Biochemistry 26*, 931−942.
Felsenfeld, G., Davies, D. R., & Rich, A. (1957) *J. Am. Chem. Soc. 79*, 2023−2024.
François, J.-C., Saison-Behmoaras, T., & Hélène, C. (1988) *Nucleic Acids Res. 16*, 11431−11440.
François, J.-C., Saison-Behmoaras, T., Barbier, C., Chassignol, M., Thuong, N. T., & Hélène, C. (1989a) *Proc. Natl. Acad. Sci. U.S.A. 86*, 9702−9706.
François, J.-C., Saison-Behmoaras, T., Thuong, N. T., & Hélène, C. (1989b) *Biochemistry 28*, 9617−9619.
Gold, B., Dange, V., Moore, M. A., Eastman, A., van der Marel, G. A., van Boom, J. H., & Hecht, S. M. (1988) *J. Am. Chem. Soc. 110*, 2347−2349.
Grigoriev, M., Praseuth, D., Robin, P., Hemar, A., Saison-Behmoaras, T., Dautry-Varsat, A., Thuong, N. T., Hélène, C., & Harel-Bellan, A. (1992) *J. Biol. Chem. 267*, 3389−3395.
Grigoriev, M., Praseuth, D., Guieysse, A. L., Robin, P., Thuong, N. T., Hélène, C., & Harel-Bellan, A. (1993) *Proc. Natl. Acad. Sci. U.S.A. 90*, 3501−3505.
Haidle, C. W., Lloyd, R. S., & Robberson, D. L. (1979) in *Bleomycin: Chemical, Biochemical and Biological Aspects* (Hecht, S. M., Ed.) pp 222−243, Springer-Verlag, New York.
Hecht, S. M. (1986) *Acc. Chem. Res. 19*, 383−391.
Hecht, S. M. (1994) *Bioconjugate Chem. 5*, 513−526.
Hecht, S. M. (1995) in *Cancer Chemotherapeutic Agents* (Foye, W. O., Ed.) pp 369−388, American Chemical Society, Washington, DC.
Hénichart, J.-P., Bernier, J.-L., Helbecque, N., & Houssin, R. (1985) *Nucleic Acids Res. 13*, 6703−6717.
Henner, W. D., Rodriguez, L. O., Hecht, S. M., & Haseltine, W. A. (1983) *J. Biol. Chem. 258*, 711−713.
Hertzberg, R. P., & Dervan, P. B. (1984) *Biochemistry 23*, 3934−3945.
Hertzberg, R. P., Caranfa, M. J., & Hecht, S. M. (1985) *Biochemistry 24*, 5285−5289.
Hertzberg, R. P., Caranfa, M. J., & Hecht, S. M. (1988) *Biochemistry 27*, 3164−3174.
Hingerty, B., Richie, R. H., Ferrel, T. L., & Turner, J. E. (1985) *Biopolymers 24*, 427−429.
Holmes, C. E., & Hecht, S. M. (1993) *J. Biol. Chem. 268*, 25909−25913.
Holmes, C. E., Carter, B. J., & Hecht, S. M. (1993) *Biochemistry 32*, 4293−4307.
Howard, F. B., Miles, H. T., Liu, K., Frazier, J., Raghunathan, G., & Sasisekharan, V. (1992) *Biochemistry 31*, 10671−10677.
Htun, H., & Dahlberg, J. E. (1988) *Science 241*, 1791−1796.
Hüttenhofer, A., Hudson, S., Noller, H. F., & Mascharak, P. K. (1992) *J. Biol. Chem. 267*, 24471−24475.
Jay, E., Seth, A. K., Rommens, J., Sood, A., & Jay, G. (1982) *Nucleic Acids Res. 10*, 6319−6329.
Johnston, B. H. (1988) *Science 241*, 1800−1804.
Kane, S. A., & Hecht, S. M. (1994) *Prog. Nucleic Acid Res. Mol. Biol. 49*, 313−352.
Kozarich, J. W., Worth, L., Jr., Frank, B. L., Christner, D. F., Vanderwall, D. E., & Stubbe, J. (1989) *Science 245*, 1396−1399.
Kross, J., Henner, W. D., Hecht, S. M., & Haseltine, W. A. (1982) *Biochemistry 21*, 4310−4318.
Kuwabara, M., Yoon, C., Goyne, T., Thederahn, T., & Sigman, D. S. (1986) *Biochemistry 25*, 7401−7408.
Kuwahara, J., & Sugiura, Y. (1988) *Proc. Natl. Acad. Sci. U.S.A. 85*, 2459−2463.
Lavery, R. (1988) in *Structure and Expression, Volume 3, DNA bending and curvature* (Olson, W. K., Sarma, M. H., Sarma, R. H., & Sundralingam, M., Eds.) pp 191−211, Adenine Press, Guilderland, NY.
Lavery, R., & Sklenar, H. (1989) *J. Biomol. Struct. Dyn. 4*, 655−667.
Le Doan, T., Perrouault, L., Praseuth, D., Habhoub, N., Decout, J. L., Thuong, N. T., Lhomme, J., & Hélène, C. (1987) *Nucleic Acids Res. 15*, 7749−7760.
Levy, M. J., & Hecht, S. M. (1988) *Biochemistry 27*, 2647−2650.
Long, E. C., Hecht, S. M., van der Marel, G. A., & van Boom, J. H. (1990) *J. Am. Chem. Soc. 112*, 5272−5276.
Macaya, R. F., Schultze, P., & Feigon, J. (1992a) *J. Am. Chem. Soc. 114*, 781−783.
Macaya, R., Wang, E., Schultze, P., Sklenar, V., & Feigon, J. (1992b) *J. Mol. Biol. 225*, 755−773.
Maher, L. J., III, Wold, B., & Dervan, P. B. (1989) *Science 245*, 725−730.
Manderville, R. A., Ellena, J. F., & Hecht, S. M. (1994) *J. Am. Chem. Soc. 116*, 10851−10852.
Manderville, R. A., Ellena, J. F., & Hecht, S. M. (1995) *J. Am. Chem. Soc. 117*, 7891−7903.
Mascharak, P. K., Sugiura, Y., Kuwahara, J., Suzuki, T., & Lippard, S. J. (1983) *Proc. Natl. Acad. Sci. U.S.A. 80*, 6795−6798.
Mirabelli, C. K., Huang, C.-H., & Crooke, S. T. (1983) *Biochemistry 22*, 300−306.
Moser, H. E., & Dervan, P. B. (1987) *Science 238*, 645−650.
Natrajan, A., & Hecht, S. M. (1993) in *Molecular Aspects of Anticancer Drug-DNA Interactions* (Neidle, S., & Waring, M. J., Eds.) Vol. 2, pp 197−242, Macmillan Press, London.
Ouali, M., Letellier, R., Adnet, F., Liquier, J., Sun, J.-S., Lavery, R., & Taillandier, E. (1993) *Biochemistry 32*, 2098−2103.
Park, Y.-W., & Breslauer, K. J. (1992) *Proc. Natl. Acad. Sci. U.S.A. 89*, 6653−6657.
Perrouault, L., Asseline, U., Rivalle, C., Thuong, N. T., Bisagni, E., Giovannangeli, C., Le Doan, T., & Hélène, C. (1990) *Nature 344*, 358−360.
Povirk, L. F., Hogan, M., & Dattagupta, N. (1979) *Biochemistry 18*, 96−101.
Povirk, L. F., Hogan, M., Dattagupta, N., & Buechner, M. (1981) *Biochemistry 20*, 665−671.
Rabow, L., Stubbe, J., Kozarich, J. W., & Gerlt, J. A. (1986) *J. Am. Chem. Soc. 108*, 7130−7131.
Saenger, W. (1984) *Principles of Nucleic Acid Structure*, Springer-Verlag, New York.
Sausville, E. A. Peisach, J., & Horwitz, S. B. (1978) *Biochemistry 17*, 2740−2746.
Sigman, D. S. (1986) *Acc. Chem. Res. 19*, 180−186.
Sikic, B. I., Rozencweig, M., & Carter, S. K., Eds. (1985) *Bleomycin Chemotherapy*, Academic Press, Orlando.
Stofer, E., & Lavery, R. (1994) *Biopolymers 34*, 337−346.
Strobel, S. A., Doucette-Stamm, L. A., Riba, L., Housman, D. E., & Dervan, P. B. (1991) *Science 254*, 1639−1642.
Stubbe, J., & Kozarich, J. W. (1987) *Chem. Rev. 87*, 1107−1136.
Sugiura, Y., & Suzuki, T. (1982) *J. Biol. Chem. 257*, 10544−10546.
Sugiyama, H., Kilkuskie, R. E., Hecht, S. M., van der Marel, G. A., & van Boom, J. H. (1985a) *J. Am. Chem. Soc. 107*, 7765−7767.
Sugiyama, H., Xu, C., Murugesan, N., & Hecht, S. M. (1985b) *J. Am. Chem. Soc. 107*, 4104−4105.
Sugiyama, H., Xu, C., Murugesan, N., Hecht, S. M., van der Marel, G. A., & van Boom, J. H. (1988) *Biochemistry 27*, 58−67.
Sun, J.-S., François, J. C., Montenay-Garestier, T., Saison-Behmoaras, T., Roig, V., Thuong, N. T., & Hélène, C. (1989) *Proc. Natl. Acad. Sci. U.S.A. 86*, 9198−9202.
Sun, J.-S., Giovannangeli, C., François, J. C., Kurfurst, R., Montenay-Garestier, T., Asseline, U., Saison-Behmoaras, T., Thuong, N. T., & Hélène, C. (1991) *Proc. Natl. Acad. Sci. U.S.A. 88*, 6023−6027.
Suzuki, T., Kuwahara, J., & Sugiura, Y. (1983) *Biochem. Biophys. Res. Commun. 117*, 916−922.
Takeshita, M., Grollman, A. P., Ohtsubo, E., & Ohtsubo, H. (1978) *Proc. Natl. Acad. Sci. U.S.A. 75*, 5983−5987.
Thuong, N. T., & Hélène, C. (1993) *Angew. Chem., Int. Ed. Engl. 32*, 666−690.
Williams, L. D., & Goldberg, I. H. (1988) *Biochemistry 27*, 3004−3011.
Wu, J. C., Kozarich, J. W., & Stubbe, J. (1983) *J. Biol. Chem. 258*, 4694−4697.
Wu, J. C., Kozarich, J. W., & Stubbe, J. (1985) *Biochemistry 24*, 7562−7568.
Wu, W., Vanderwall, D. E., Stubbe, J., Kozarich, J. W., & Turner, C. J. (1994) *J. Am. Chem. Soc. 116*, 10843−10844.
Yoon, C., Privé, G. G., Goodsell, D. S., & Dickerson, R. E. (1988) *Proc. Natl. Acad. Sci. U.S.A. 85*, 6332−6336.

BI9519462